JBC Papers in Press. Published on August 14, 2019 as Manuscript AC119.009749 The latest version is at http://www.jbc.org/cgi/doi/10.1074/jbc.AC119.009749

The ghrelin O-acyltransferase structure reveals a catalytic channel for transmembrane hormone acylation

Maria B. Campaña^{#,1}, Flaviyan Jerome Irudayanathan^{#,2}, Tasha R. Davis¹, Kayleigh R. McGovern-Gooch^{1,†}, Rosemary Loftus¹, Mohammad Ashkar¹, Najae Escoffery¹, Melissa Navarro¹, Michelle A. Sieburg¹, Shikha Nangia^{2,3*}, and James L. Hougland^{1,3*}

From the ¹Department of Chemistry, Syracuse University, Syracuse, NY 13244;

Running Title: *Molecular structure of GOAT*

†Present address: Department of Chemistry and Biochemistry, University of the Sciences, Philadelphia, PA 19104

Shikha Nangia: Department of Biomedical and Chemical Engineering, Syracuse University, Syracuse, NY 13244; snangia@syr.edu; Tel. (315) 443-0571

James L. Hougland: Department of Chemistry, Syracuse University, Syracuse, NY 13244; hougland@syr.edu; Tel. (315) 443-1134

Keywords: Protein structure prediction, membrane bound O-acyltransferase (MBOAT), integral membrane protein, protein acylation, ghrelin O-acyltransferase (GOAT), computational modeling, structural biology, co-evolutionary constraint, posttranslational modification

ABSTRACT

Integral membrane proteins represent a large and diverse portion of the proteome and are often recalcitrant to purification, impeding studies essential for understanding protein structure and combining co-evolutionary function. By constraints and computational modeling with biochemical validation through site-directed mutagenesis and enzyme activity assays, we demonstrate here a synergistic approach to structurally model purification-resistant topologically complex integral membrane proteins. We report the first structural model of a eukaryotic membrane-bound O-acyltransferase (MBOAT), ghrelin O-acyltransferase (GOAT), which modifies the metabolism-regulating hormone ghrelin. Our structure, generated in the absence of any experimental structural data, revealed an unanticipated strategy transmembrane protein acylation with catalysis occurring in an internal channel connecting the endoplasmic reticulum (ER) lumen and cytoplasm. This finding validated the power of our approach to generate predictive structural models for other experimentally challenging integral membrane proteins. Our results illuminate novel aspects of membrane protein function and represent key steps for advancing structure-guided inhibitor design to target therapeutically important but experimentally intractable membrane proteins.

Integral membrane proteins represent a large and essential portion of the proteome, including a growing number of enzymes, receptors, and transporters that serve as desirable drug targets.(1,2) However, these proteins often prove recalcitrant to purification and structural analysis due to their hydrophobic nature and reliance on interactions with lipid bilayers for both stability and activity.(3,4) We report here a synergistic approach to develop a structural model of a topologically complex integral membrane protein by combining co-evolutionary contact constraints and computational modeling with biochemical validation. Building solely upon the protein's

²Department of Biomedical and Chemical Engineering, Syracuse University, Syracuse, NY 13244;

³Syracuse Biomaterials Institute, Syracuse University, Syracuse, NY 13244

^{*}These authors contributed equally to the work

^{*}To whom correspondence should be addressed:

primary sequence and a biochemical assay for its function, the approach provides an accessible and efficient route to build structural models of intractable membrane protein targets.

We demonstrate this approach by developing a structural model for ghrelin O-acyltransferase (GOAT), a member of the membrane bound Oacyltransferase (MBOAT) enzyme family responsible for octanoylation of the peptide hormone ghrelin (Fig. 1).(5,6) One of three protein-modifying MBOAT family members alongside Hedgehog acyltransferase (Hhat) and Porcupine (Porcn),(7-9) GOAT plays a central role in regulating energy homeostasis and metabolism through octanovlated ghrelindependent signaling pathways.(10) While the unique chemistry and biology of ghrelin and GOAT have inspired continued efforts to target this system for therapeutic benefit, the inability to purify active GOAT and determine its structure has hampered progress towards this goal.(11-13) In this work, we report the first structural model for a eukaryotic MBOAT family member. Our human GOAT (hGOAT) structure is highly consistent with a recently reported crystal structure for the bacterial MBOAT homolog Dalanyl transferase DltB.(14) Our structure suggests a novel strategy for solving the topological challenge presented transmembrane protein acylation where protein targets and co-substrates are separated by a cellular membrane. In an unanticipated mechanism, ghrelin octanovlation occurs in an internal channel within hGOAT without the octanoyl-CoA donor being transported into the endoplasmic reticulum (ER) lumen. The availability of this therapeutically interesting enzyme's structure opens the door to the structure-guided design of inhibitors targeting GOAT and other MBOAT family members. Looking beyond the MBOATs, our success in modeling GOAT and predicting specific proteinligand interactions validates the power of our approach for creating molecular models for other experimentally challenging integral membrane proteins.

Results and Discussion Computational model for human GOAT structure

In generating our hGOAT structural model, we utilized state-of-the-art co-evolutionary contact predictions with computational protein folding and structure optimization methods (Supp. Fig. S1).(15,16) Coevolutionary contact analysis exploits the tendency of residues interacting with each other within folded proteins to co-evolve to maintain energetically beneficial interactions.(17-19) Analysis of many protein sequences employing a multiple-sequence alignment identifies pairs of co-evolving residues, from which it is inferred that these residues lie in proximity to each other. Assigning pairs of residues as co-evolving supports assignment of spatial interactions between them, providing constraints that can define major features protein structure. metagenomics protein databases, we generated a multiple-sequence alignment to predict residues that are potentially in contact (defined as C_{β} - C_{β} < 8Å) with each other in the folded structure of hGOAT (Supp. Info. File S1).(15,20) This set of contacts (Supp. Info. File S2), represented by the contact map (Fig. 1c and Supp. Fig. S2), guided our hGOAT structural modeling.(17,20,21) Experimental information on the membrane topology of mouse GOAT and co-evolutionary contact constraints were iteratively combined in protein folding simulations to generate ~30,000 potential hGOAT structures.(11,17,22) The generated structures were clustered, and the lowest energy structures that satisfied the contact map were isolated (Supp. Fig. S3).(22) Representative structures from the top five clusters were then subjected to further structural refinement to yield the optimal hGOAT model.(23) The optimal model was embedded in a lipid membrane and subjected to structural relaxation in explicit solvent using all-atom molecular dynamics simulations.(24-26) This simulation used an ER-mimetic lipid bilayer to ensure optimization of hydrophobic protein-lipid interactions.(27)

Features of the human GOAT structure

Our computationally-derived structure for hGOAT is consistent with the previously reported topological model of the mouse GOAT ortholog containing a total of eleven transmembrane helices with slightly altered helix boundaries (Fig. 1a),(11) indicating the two sets of

constraints from our coevolutionary contact analysis and previous topological studies support a common hGOAT structural model. To determine how strongly our hGOAT structure depends on the experimental topological constraints from mouse GOAT,(11) we excluded these constraints and repeated our analysis which generated an identical hGOAT membrane topology. This indicates co-evolutionary contact constraints alone are sufficient to predict the membrane topology of hGOAT, suggesting this approach for topology modeling of integral membrane proteins to complement established algorithms for predicting membrane protein topology.

Ramachandran analysis indicates 92.4% (400/433) of hGOAT residues lie in favored (98%) regions, 98.2% (425/433) lie in allowed (>99.8%) regions, and 1.9% (8/433) were outliers (Supp. Fig. S4).(28) The enzyme forms an ellipsoidal cone composed of transmembrane helices, with the narrow end facing the ER lumen The exposed ends of five 1d). transmembrane helices (TM1, TM4, TM5, TM7, and TM11) converge to form a pore through which the interior of hGOAT is connected to the ER lumen. At the cytoplasmic membrane interface, the predicted cytoplasmic loops fold up to form a core region bounded by the lipidcontacting perimeter helices. As a result, there is minimal cytoplasmic exposure of hGOAT residues beyond the plane of the membrane.

The hGOAT structure contains a contiguous internal channel through the enzyme core that transits from the ER lumen space to the cytoplasm (Fig. 1e). The channel is bent within hGOAT, with the restriction formed by the Cterminal end of helix TM8 and N-terminal end of TM9. This positions an absolutely conserved histidine residue (H338) in direct contact with the internal channel, (7) consistent with proposals for this histidine to serve as a general base for catalyzing ghrelin acylation. Following completion of our hGOAT structure and during subsequent biochemical validation experiments (described below), the release of a crystal structure for the bacterial MBOAT DltB alanyl transferase provided an independent basis for comparison and validation of our hGOAT structure.(14) The H338 residue in hGOAT closely matches the location of the analogous

histidine residue (H336) in the DltB structure (Fig. 1f).(5,14) Further comparison of the hGOAT model and the DltB structure reveals remarkable similarities in overall topology and structure, with an TM-Score of 0.6 and RMSD of 2.23 Å for ~100 aligned conserved residues between the structural models for these distantly related MBOAT family members (12.3% sequence identity, 26.8% sequence similarity, E-Value 2.7x10⁻⁸ and bit score 48.7; Supp. Figs. S5-S6, and Table S1).(29) However, the low overall homology between DltB and hGOAT leads to very poor structure prediction for nonhomologous sequence positions as would be expected for this type of comparison. The demonstrated ability of our hGOAT modeling based on coevolutionary contact restraints to arrive at the same protein fold as DltB, in the absence of any experimental structural information, underscores the power of this approach to accurately predict protein structures.

Mutagenesis analysis of hGOAT structural model

To validate our computational hGOAT structural model biochemically, we mutated approximately 10% of the residues within hGOAT to alanine and determined the impact of these mutations on hGOAT octanoylation activity in a peptide-based acylation assay (Fig. 2 and Supp. Fig. S7).(30,31) These 42 alanine mutations were spread across a range of amino acids and degrees of conservation, with the majority of sites chosen conserved at >75% among GOAT orthologs (Supp. Data S3). In narrowing the pool of mutations to ~40 positions, residues with surface-exposed side chains were deemphasized compared to residues predicted to lie within the enzyme interior. Approximately half of the mutation sites were selected based on the residue's side chain contacting the internal void, as we propose this channel will likely contain the substrate binding sites and catalytic residues within hGOAT.

In this pool of alanine mutants, we observed a range of activities from near/above wild type ghrelin octanoylation activity to complete loss of detectable activity (Supp. Table S2 and Fig. S8). When mapped onto the hGOAT structural model, mutations leading to a marked decline (>3-fold, purple) or loss of enzyme activity (red) appear

clustered within the core of hGOAT (Fig. 2). For quantitative analysis of the impact of these mutations, we determined whether alanine mutagenesis of residues contacting the internal void is more likely to yield reduced enzyme activity compared to non-void contacting mutations. Within the pool of mutations, the void-contacting alanine mutations significantly more likely to result in loss of enzyme activity (p<0.03, Fig. 2d). This mutation activity mapping defines a functionally essential core within hGOAT and expands the number of residues within hGOAT known to be required for enzyme activity.(5,6,11)

The octanoyl-CoA binding site within hGOAT

We expect the octanoyl-CoA acyl donor to enter the hGOAT active site through interaction with the cytoplasmic face of the enzyme, based on the availability of acyl-CoAs within the cell. When docked into our hGOAT model, octanoyl-CoA binds to hGOAT through interactions of both its coenzyme A and octanoyl chain regions with residues in TM6, the TM7-TM8 connecting loop, TM8, and TM9 (Fig. 3). In the docked complex, the coenzyme A portion forms both polar and nonpolar interactions with multiple hGOAT residues while remaining exposed to the cytoplasm (Fig. 3a-b). The phosphoadenosine group binds into a discrete pocket while the phosphopantetheine chain is in contact with multiple polar amino acid side chains (Fig. 3c-e). Among these CoA-contacting amino acids, all alanine mutations examined except one lead to a loss of hGOAT activity.

In the docked hGOAT:octanoyl-CoA structure, the acyl chain of octanoyl-CoA makes a sharp turn and penetrates upward into the interior of hGOAT following a channel that terminates at W351 (Fig. 3c-e). Given the unique preference of hGOAT for an octanovl acvl donor, (6, 13, 32) we examined alanine mutagenesis of predicted contacts within this acvl binding pocket to determine the impact of those mutations on hGOAT acyl donor selectivity. As alanine mutagenesis would provide additional space within the acyl binding site, we determined the ability of hGOAT alanine variants to accept twelve carbon (lauryl-CoA) and fourteen carbon (myristoyl-CoA) acyl donors in place of octanoyl CoA. The wild type enzyme and the majority of

hGOAT alanine variants exhibited the expected preference for an eight carbon acyl donor, but alanine mutagenesis of W351 and F331 resulted in loss of appreciable reactivity with octanovl-CoA but engendered new activity with the longer acyl donors (Fig. 3f and Supp. Fig. S9). The F331A variant gained activity with the C12 donor while W351A hGOAT could acylate a ghrelinderived peptide with both C12 and C14 acyl chains. This altered selectivity supports the modeled positions of W351 and F331 as forming the end of the acyl binding pocket. The altered preference for longer acyl donors by the F331A and W351A variants was also observed in a direct competition assay where hGOAT variants were provided acyl donors ranging from six to twelve carbons. (Fig. 3g) This altered selectivity was not observed for any other alanine variants with detectable ghrelin acylation activity (Supp. Fig. S10). Acyl donor reengineering upon targeted alanine mutagenesis localizes F331 and W351 to the distal end of the acyl donor binding site within hGOAT and provides further biochemical validation of our hGOAT structural model.

While structural studies play a central role in developing our understanding of protein function, the limited availability of integral membrane proteins within structural databases creates a particularly acute challenge for structurally modeling these proteins.(33) In this work, we demonstrate the development and validation of a structural model for an integral membrane protein that leverages bioinformatics constraints from coevolutionary contact analysis and model evaluation by biochemical analysis while circumventing the requirement of protein purification.

Our model provides indispensable and novel insights into several long-standing questions regarding the mechanism for MBOAT-catalyzed transmembrane protein acylation. topological separation of two essential conserved residues, H338 and N307, is explained by these two residues playing roles in distinct aspects of GOAT activity. The location of H338 within the central channel of GOAT, identical to the position observed for the analogous histidine in DltB₃(14) is consistent with this residue acting as a general base to activate the ghrelin serine hydroxyl side chain for octanovl transfer. In contrast, our hGOAT:octanovl-CoA model

implicates N307 in the binding site for the acyl donor. Based on our models of hGOAT and the hGOAT:octanovl-CoA complex, we propose that hGOAT catalyzes transmembrane acylation of ghrelin by binding both substrates within the hGOAT internal channel and "handing off" the octanoyl group from CoA to ghrelin within this channel (Fig. 4). While many aspects of this proposed pathway — such as the ghrelin binding site and location of catalytic residues — remain to be functionally validated by ongoing studies, the established ability of our hGOAT model to guide biochemical efficiently studies demonstrates a novel approach to advance investigations of similar membrane proteins that are intractable to current structural approaches.

Experimental Procedures

Co-evolutionary contact analysis of hGOAT

A multiple sequence alignment (MSA) was performed with the hGOAT sequence against the UNIREF90 database utilizing the jackhmmer tool.(34) The MSA parameters were set to eight iterative searches (n=8) with an e-value threshold of 1x10⁻⁴⁰. The resulting alignment was filtered to exclude highly similar sequences using the HHfilter tool with 90% identity and 75% sequence coverage cut-offs. This MSA was used as the input for the hmmbuild tool to construct a hidden Markov model (hmm) curated specifically for the MSA,(35) which would represent the consensus sequence of hGOAT and its closest homologs. This hmm was then utilized to search against a master database that included uniref100 and metagenome database (metaclust 2018 01) using the hmmsearch tool with a bit score cut-off of 27.(15,21) The resulting MSA was filtered again using the HHfilter tool with 90% identity and 75% sequence coverage against hGOAT. Furthermore, sequences with unidentified amino acids (X, this is to accommodate for RaptorX) and sequence positions with >50% gaps were also filtered from the MSA using trimAL.(36) The resulting MSA for hGOAT was primarily used to perform co-evolutionary contact analysis using the RaptorX server and GREMLIN.(15,17,20,37) The resulting contact maps are provided as Figure 1b (RaptorX) in the text and Supp. Fig. S2 (GREMLIN). The resulting MSA had a M_{eff} - $0.8/\sqrt{N}$ of 551.7 which is greater than the recommended value of 64 for reliable model prediction using co-evolutionary contacts.(15,17) These contacts were used to guide the hGOAT folding. The MSA analysis and curations were performed using in-house python scripts and conkit python library.(38)

Folding simulations

The folding simulations were performed in two stages. In both stages, contact restraints were used and the models were iteratively clustered, refined and scored based on their overall backbone energy. Full details of the folding simulation protocols and software are provided in the Supp. Information.

Refinement and relaxation using molecular dynamics

The optimized hGOAT model from stage 2 was oriented with respect to a membrane bilayer using the PPM server.(25) The calculated hydrophobic thickness of the hGOAT structural model is 25.2 \pm 2.4 Å and the tilt angle of 3° relative to the membrane normal vector. The oriented protein was then embedded in a ER-mimetic lipid bilayer (1:1 dipalmitoylphosphatidylcholine(DPPC) : dioleovl phosphatidylcholine(DOPC)) using the CHARMM-GUI webserver and subject to an allatom equilibration at 310.15 K in explicit solvent and 150 mM NaCl counter ions.(24,39) The simulation was carried out for 500 ns using GROMACS 2016.4 and the structural deviations were monitored.(40) The equilibrated structure was isolated and utilized for prediction of internal channels and docking studies.

Molecular docking and relaxation of octanoyl-CoA:hGOAT complex

To build a model of the octanoyl-CoA•hGOAT bound complex, we performed docking using Autodock Vina implemented in the YASARA software suite;(41,42) full details of the docking procedure are provided in the Supp. Information.

General experimental methods

Data plotting and curve fitting were carried out with Kaleidagraph (Synergy Software, Reading, PA, USA). Membrane topology schematics were generated using Protter (http://wlab.ethz.ch/protter/start/),(43) and structural figures were generated using

Chemdraw Prime 15.1 and PyMol. Hexanoyl coenzyme A (hexanoyl-CoA, free acid) (Crystal Chem Inc.), octanovl coenzyme A (octanovl-CoA, free acid) (AdventBio), decanovl coenzyme A (decanoyl-CoA, free acid) (Crystal Chem Inc.), lauroyl coenzyme A (lauroyl-CoA, dodecanoyl-CoA, free acid) (Crystal Chem Inc.), and mvristovl coenzvme Α (mvristovl-CoA. tetradecanoyl-CoA, free acid) (Crystal Chem Inc.) were solubilized to 5 mM in 10 mM Tris-HCl (pH 7.0), aliquoted into low-adhesion microcentrifuge tubes, and stored at -80 °C. arachidonyl fluorophosphonate Methoxy (MAFP) was purchased from Cayman Chemical (Ann Arbor, MI) and solubilized with dimethyl sulfoxide (DMSO). Unlabeled GSSFLC_{NH2} peptide was synthesized by Sigma-Genosys (The Woodlands, solubilized TX), in acetonitrile:H₂O, and stored at -80 °C. Acrylodan (Anaspec) for peptide substrate labeling was solubilized in acetonitrile with the stock concentration determined by absorbance at 393 nm in methanol ($\varepsilon_{393} = 18,483 \text{ M}^{-1}\text{cm}^{-1}$, per the manufacturer's data sheet). GSSFLC_{NH2} peptide concentrations were determined by reaction of with 5,5'-dithiobis(2cysteine thiol nitrobenzoic acid) and absorbance at 412 nm. using $\varepsilon_{412} = 14{,}150 \text{ M}^{-1} \text{ cm}^{-1}.(44)$

Peptide substrate fluorescent labeling

The GSSFLC_{NH2} peptide substrate used in the hGOAT acylation assay was fluorescently labeled and purified using previously reported protocols.(30,45,46) The concentration of acrylodan labeled GSSFLC_{NH2} was calculated using absorbance of acrylodan at 360 nm (ϵ = 13,300 M⁻¹cm⁻¹).(30,47)

Construction of hGOAT mutants

Site-directed mutagenesis was performed onour previously reported hGOAT expression construct as described in the Supp. Information.(30) This construct was commercially synthesized by Integrated DNA Technologies (Coralville, IA) containing a C-terminal FLAG epitope tag, a polyhistidine (His₆) tag, and 3x human influenza hemagglutinin (HA) tags appended downstream of a TEV protease site.(48)

Expression and enrichment of hGOAT in membrane protein fractions

hGOAT wildtype and mutants were expressed in insect (Sf9) cell membrane fractions using previously published procedures. (13,30,46,49)

hGOAT expression analysis by anti-FLAG Western Blot

Expression of hGOAT was determined by anti-FLAG Western blotting using published protocols (Supp. Fig. S7).(46) Each gel contained an empty vector (EV) microsomal protein as negative control and amino-terminal FLAG-BAP Fusion protein as a positive control (Millipore Sigma, P7582-100UG, 1:150 dilution, 30 μL total volume).

Following electrophoretic separation and transfer to a PVDF membrane, the membrane was probed with a Flag antibody (HRP-conjugated DYKDDDDK Tag Antibody, Invitrogen catalog number PA1-984B-HRP, 1:1000 dilution, 10 mL total volume) in 5% nonfat milk in TBST buffer overnight at 4 °C. The membrane was treated with West Pico Chemiluminescent substrate-imaging reagent (Thermo Scientific) followed by imaging on a ChemiDoc XRS+ gel documentation system (BioRad).

hGOAT activity assay - standard reaction conditions

hGOAT activity assays under standard conditions were performed with 50 µg of membrane protein, 1.5 µM fluorescent peptide substrate, 300 µM octanoyl-CoA, 1 µM MAFP, and 50 µM HEPES pH 7.0 in a total volume of 50 µL as previously described.(46) All components except for the peptide and acyl-CoA substrates were incubated at room temperature for 30 minutes prior to reaction initiation by addition of peptide and acyl-CoA substrates. Reactions were incubated at room temperature for 2 hour in the dark and then stopped by addition of 50 µL of 20% acetic acid in isopropanol. Reaction solutions were clarified and analyzed by reverse phase HPLC.(46) Substrate and acylated products were detected by fluorescence (λ_{ex} 360 nm, λ_{em} 485 nm), with the substrate eluting with a retention time of 5-6 minutes and the octanovlated peptide eluting with a retention time of 11-12 minutes. Chromatogram analysis and peak integration was performed Chemstation using for LC (Agilent Technologies).(30) Product conversion was calculated by dividing the integrated fluorescence

for the product peak by the total integrated peptide fluorescence (substrate and product) in each run. Percent activity for each hGOAT mutant was calculated by normalizing the product conversion for the mutant to that of wild type hGOAT in a reaction run in parallel on the same day using the same reagents.

Statistical analysis of hGOAT alanine variant reactivity

Full details of hGOAT alanine variant statistical testing using a Wilcoxon signed-rank test (n=42, test statistic W=294.5, p-value = 0.02978) are in provided in the Supp. Information, including the R script utilized.(50)

Single acyl donor reactivity assay

To determine the reactivity of hGOAT variants with different length acyl donors, hGOAT activity was measured in the presence of 100 μM of a single acyl donor (octanoyl-CoA, lauryl (dodecanoyl)-CoA, or myristoyl (tetradecanoyl)-CoA). Characteristic retention times for each acylated form of the peptide substrate provided confirmation of the nature of the attached acyl chain, with dodecanoyl-GSSFLC_{AcDan} eluting at $\sim\!17$ minutes and tetradecanoyl- GSSFLC_{AcDan} eluting at $\sim\!19$ minutes. For each acyl donor, relative activity was calculated normalized to the highest activity observed across the panel of wildtype hGOAT and hGOAT variants.

Acyl donor competition assay

To determine the relative preference of each hGOAT variant for acyl donors ranging from six to twelve carbons, hGOAT activity was measured in the presence of 100 μM each of four potential acyl donors (hexanoyl-CoA, octanoyl-CoA, decanoyl-CoA, and lauryl (dodecanoyl)-CoA). Each potential product peak was assigned by retention time compared to a standard reaction containing only one acyl donor for each potential product. Competition experiments including myristoyl-CoA were unsuccessful, potentially due to low critical micelle concentration (CMC) for this acyl donor lying near 100 μM.(51)

Acknowledgements: The authors thank Profs. Jason Fridley and John Chisholm (Syracuse University) for assistance with statistical analysis and figure generation. The authors also thank Prof. Jinbo Xu (Toyota Technological Institute at Chicago), Prof. Sergey Ovchinnikov (Harvard University), and Prof. Badri Adhikari (University of Missouri–St. Louis) for their advice regarding computational modeling.

Conflict of Interest: The authors declare that they have no conflicts of interest with the contents of this article.

References

- 1. Rask-Andersen, M., Almen, M. S., and Schioth, H. B. (2011) Trends in the exploitation of novel drug targets. *Nat Rev Drug Discov* **10**, 579-590
- 2. Overington, J. P., Al-Lazikani, B., and Hopkins, A. L. (2006) How many drug targets are there? *Nat Rev Drug Discov* **5**, 993-996
- 3. Stansfeld, P. J., Goose, J. E., Caffrey, M., Carpenter, E. P., Parker, J. L., Newstead, S., and Sansom, M. S. (2015) Memprotmd: Automated insertion of membrane protein structures into explicit lipid membranes. *Structure* **23**, 1350-1361
- 4. Bill, R. M., Henderson, P. J., Iwata, S., Kunji, E. R., Michel, H., Neutze, R., Newstead, S., Poolman, B., Tate, C. G., and Vogel, H. (2011) Overcoming barriers to membrane protein structure determination. *Nat Biotechnol* **29**, 335-340
- 5. Yang, J., Brown, M. S., Liang, G., Grishin, N. V., and Goldstein, J. L. (2008) Identification of the acyltransferase that octanoylates ghrelin, an appetite-stimulating peptide hormone. *Cell* **132**, 387-396
- 6. Gutierrez, J. A., Solenberg, P. J., Perkins, D. R., Willency, J. A., Knierman, M. D., Jin, Z., Witcher, D. R., Luo, S., Onyia, J. E., and Hale, J. E. (2008) Ghrelin octanoylation mediated by an orphan lipid transferase. *Proc Natl Acad Sci U S A* **105**, 6320-6325
- 7. Hofmann, K. (2000) A superfamily of membrane-bound o-acyltransferases with implications for wnt signaling. *Trends Biochem Sci* **25**, 111-112
- 8. Masumoto, N., Lanyon-Hogg, T., Rodgers, U. R., Konitsiotis, A. D., Magee, A. I., and Tate, E. W. (2015) Membrane bound o-acyltransferases and their inhibitors. *Biochem Soc Trans* **43**, 246-252
- 9. Resh, M. D. (2016) Fatty acylation of proteins: The long and the short of it. *Prog Lipid Res* **63**, 120-131
- Muller, T. D., Nogueiras, R., Andermann, M. L., Andrews, Z. B., Anker, S. D., Argente, J., Batterham, R. L., Benoit, S. C., Bowers, C. Y., Broglio, F., Casanueva, F. F., D'Alessio, D., Depoortere, I., Geliebter, A., Ghigo, E., Cole, P. A., Cowley, M., Cummings, D. E., Dagher, A., Diano, S., Dickson, S. L., Dieguez, C., Granata, R., Grill, H. J., Grove, K., Habegger, K. M., Heppner, K., Heiman, M. L., Holsen, L., Holst, B., Inui, A., Jansson, J. O., Kirchner, H., Korbonits, M., Laferrere, B., LeRoux, C. W., Lopez, M., Morin, S., Nakazato, M., Nass, R., Perez-Tilve, D., Pfluger, P. T., Schwartz, T. W., Seeley, R. J., Sleeman, M., Sun, Y., Sussel, L., Tong, J., Thorner, M. O., van der Lely, A. J., van der Ploeg, L. H., Zigman, J. M., Kojima, M., Kangawa, K., Smith, R. G., Horvath, T., and Tschop, M. H. (2015) Ghrelin. *Mol Metab* 4, 437-460
- 11. Taylor, M. S., Ruch, T. R., Hsiao, P. Y., Hwang, Y., Zhang, P., Dai, L., Huang, C. R., Berndsen, C. E., Kim, M. S., Pandey, A., Wolberger, C., Marmorstein, R., Machamer, C., Boeke, J. D., and Cole, P. A. (2013) Architectural organization of the metabolic regulatory enzyme ghrelin o-acyltransferase. *J Biol Chem* **288**, 32211-32228
- 12. Taylor, M. S., Dempsey, D. R., Hwang, Y., Chen, Z., Chu, N., Boeke, J. D., and Cole, P. A. (2015) Mechanistic analysis of ghrelin-o-acyltransferase using substrate analogs. *Bioorg Chem* **62**, 64-73
- Darling, J. E., Zhao, F., Loftus, R. J., Patton, L. M., Gibbs, R. A., and Hougland, J. L. (2015) Structure-activity analysis of human ghrelin o-acyltransferase reveals chemical determinants of ghrelin selectivity and acyl group recognition. *Biochemistry* **54**, 1100-1110
- 14. Ma, D., Wang, Z., Merrikh, C. N., Lang, K. S., Lu, P., Li, X., Merrikh, H., Rao, Z., and Xu, W. (2018) Crystal structure of a membrane-bound o-acyltransferase. *Nature* **562**, 286-290
- 15. Ovchinnikov, S., Park, H., Varghese, N., Huang, P. S., Pavlopoulos, G. A., Kim, D. E., Kamisetty, H., Kyrpides, N. C., and Baker, D. (2017) Protein structure determination using metagenome sequence data. *Science* **355**, 294-298
- 16. Marks, D. S., Hopf, T. A., and Sander, C. (2012) Protein structure prediction from sequence variation. *Nat Biotechnol* **30**, 1072-1080
- 17. Ovchinnikov, S., Kinch, L., Park, H., Liao, Y., Pei, J., Kim, D. E., Kamisetty, H., Grishin, N. V., and Baker, D. (2015) Large-scale determination of previously unsolved protein structures using evolutionary information. *Elife* 4, e09248

- 18. Hopf, T. A., Scharfe, C. P., Rodrigues, J. P., Green, A. G., Kohlbacher, O., Sander, C., Bonvin, A. M., and Marks, D. S. (2014) Sequence co-evolution gives 3d contacts and structures of protein complexes. *Elife* **3**, e03430
- 19. Nicoludis, J. M., and Gaudet, R. (2018) Applications of sequence coevolution in membrane protein biochemistry. *Biochim Biophys Acta Biomembr* **1860**, 895-908
- Wang, S., Sun, S., and Xu, J. (2018) Analysis of deep learning methods for blind protein contact prediction in casp12. *Proteins*, Suppl 1:67-77
- 21. Steinegger, M., and Soding, J. (2018) Clustering huge protein sequence sets in linear time. *Nat Commun* **9**, 2542
- 22. Adhikari, B., and Cheng, J. (2018) Confold2: Improved contact-driven ab initio protein structure modeling. *BMC Bioinformatics* **19**, 22
- 23. Yang, J., Yan, R., Roy, A., Xu, D., Poisson, J., and Zhang, Y. (2015) The i-tasser suite: Protein structure and function prediction. *Nat Methods* **12**, 7-8
- 24. Huang, J., Rauscher, S., Nawrocki, G., Ran, T., Feig, M., de Groot, B. L., Grubmuller, H., and MacKerell, A. D., Jr. (2017) Charmm36m: An improved force field for folded and intrinsically disordered proteins. *Nat Methods* **14**, 71-73
- 25. Lomize, M. A., Pogozheva, I. D., Joo, H., Mosberg, H. I., and Lomize, A. L. (2012) Opm database and ppm web server: Resources for positioning of proteins in membranes. *Nucleic Acids Res* **40**, D370-376
- 26. Irudayanathan, F. J., Trasatti, J. P., Karande, P., and Nangia, S. (2016) Molecular architecture of the blood brain barrier tight junction proteins--a synergistic computational and in vitro approach. *J Phys Chem B* **120**, 77-88
- 27. Rajagopal, N., Irudayanathan, F. J., and Nangia, S. (2019) Palmitoylation of claudin-5 proteins influences their lipid domain affinity and tight junction assembly at the blood-brain barrier interface. *J Phys Chem B* **123**, 983-993
- 28. Chen, V. B., Arendall, W. B., 3rd, Headd, J. J., Keedy, D. A., Immormino, R. M., Kapral, G. J., Murray, L. W., Richardson, J. S., and Richardson, D. C. (2010) Molprobity: All-atom structure validation for macromolecular crystallography. *Acta Crystallogr D Biol Crystallogr* **66**, 12-21
- 29. Xu, J., and Zhang, Y. (2010) How significant is a protein structure similarity with tm-score = 0.5? *Bioinformatics* **26**, 889-895
- 30. Darling, J. E., Prybolsky, E. P., Sieburg, M., and Hougland, J. L. (2013) A fluorescent peptide substrate facilitates investigation of ghrelin recognition and acylation by ghrelin o-acyltransferase. *Anal Biochem* **437**, 68-76
- 31. McGovern-Gooch, K. R., Rodrigues, T., Darling, J. E., Sieburg, M. A., Abizaid, A., and Hougland, J. L. (2016) Ghrelin octanoylation is completely stabilized in biological samples by alkyl fluorophosphonates. *Endocrinology* **157**, 4330-4338
- 32. Hougland, J. L. (2019) Ghrelin octanoylation by ghrelin o-acyltransferase: Unique protein biochemistry underlying metabolic signaling. *Biochem Soc Trans* **47**, 169-178
- 33. White, S. (2019) Membrane proteins of known 3d structure. http://blanco.biomol.uci.edu/mpstruc/.
- 34. Johnson, L. S., Eddy, S. R., and Portugaly, E. (2010) Hidden markov model speed heuristic and iterative hmm search procedure. *BMC Bioinformatics* **11**, 431
- 35. Remmert, M., Biegert, A., Hauser, A., and Soding, J. (2011) Hhblits: Lightning-fast iterative protein sequence searching by hmm-hmm alignment. *Nat Methods* **9**, 173-175
- 36. Capella-Gutierrez, S., Silla-Martinez, J. M., and Gabaldon, T. (2009) Trimal: A tool for automated alignment trimming in large-scale phylogenetic analyses. *Bioinformatics* **25**, 1972-1973
- Wang, S., Li, Z., Yu, Y., and Xu, J. (2017) Folding membrane proteins by deep transfer learning. *Cell Syst* 5, 202-211 e203
- 38. Simkovic, F., Thomas, J. M. H., and Rigden, D. J. (2017) Conkit: A python interface to contact predictions. *Bioinformatics* **33**, 2209-2211
- 39. Lee, J., Cheng, X., Swails, J. M., Yeom, M. S., Eastman, P. K., Lemkul, J. A., Wei, S., Buckner, J., Jeong, J. C., Qi, Y., Jo, S., Pande, V. S., Case, D. A., Brooks, C. L., 3rd, MacKerell, A. D., Jr.,

- Klauda, J. B., and Im, W. (2016) Charmm-gui input generator for namd, gromacs, amber, openmm, and charmm/openmm simulations using the charmm36 additive force field. *J Chem Theory Comput* **12**, 405-413
- 40. Abraham, M. J., Murtola, T., Schulz, R., Pall, S., Smith, J. C., Hess, B., and Lindahl, E. (2015) Gromacs: High performance molecular simulations through multi-level parallelism from laptops to supercomputers. *SoftwareX* **1-2**, 19-25
- 41. Seeliger, D., and de Groot, B. L. (2010) Ligand docking and binding site analysis with pymol and autodock/vina. *J Comput Aided Mol Des* **24**, 417-422
- 42. Trott, O., and Olson, A. J. (2010) Autodock vina: Improving the speed and accuracy of docking with a new scoring function, efficient optimization, and multithreading. *J Comput Chem* **31**, 455-461
- 43. Omasits, U., Ahrens, C. H., Muller, S., and Wollscheid, B. (2014) Protter: Interactive protein feature visualization and integration with experimental proteomic data. *Bioinformatics* **30**, 884-886
- 44. Riddles, P. W., Blakeley, R. L., and Zerner, B. (1979) Ellman's reagent: 5,5'-dithiobis(2-nitrobenzoic acid)--a reexamination. *Anal Biochem* **94**, 75-81
- 45. Tricerri, M. A., Behling Agree, A. K., Sanchez, S. A., and Jonas, A. (2000) Characterization of apolipoprotein a-i structure using a cysteine-specific fluorescence probe. *Biochemistry* **39**, 14682-14691
- 46. Sieburg, M. A., Cleverdon, E. R., and Hougland, J. L. (2019) Biochemical assays for ghrelin acylation and inhibition of ghrelin o-acyltransferase. *Methods Mol Biol* **2009**, 227-241
- 47. Post, P. L., Trybus, K. M., and Taylor, D. L. (1994) A genetically engineered, protein-based optical biosensor of myosin ii regulatory light chain phosphorylation. *J Biol Chem* **269**, 12880-12887
- 48. Roth, A. F., Feng, Y., Chen, L., and Davis, N. G. (2002) The yeast dhhc cysteine-rich domain protein akr1p is a palmitoyl transferase. *J Cell Biol* **159**, 23-28
- 49. Wellman, M. K., Patterson, Z. R., MacKay, H., Darling, J. E., Mani, B. K., Zigman, J. M., Hougland, J. L., and Abizaid, A. (2015) Novel regulator of acylated ghrelin, cf801, reduces weight gain, rebound feeding after a fast, and adiposity in mice. *Front Endocrinol (Lausanne)* **6**, 144
- 50. Team, R. C. (2018) R: A language and environment for statistical computing. R Foundation for Statistical Computing, Vienna, Austria
- 51. Smith, R. H., and Powell, G. L. (1986) The critical micelle concentration of some physiologically important fatty acyl-coenzyme a's as a function of chain length. *Arch Biochem Biophys* **244**, 357-360
- 52. Chovancova, E., Pavelka, A., Benes, P., Strnad, O., Brezovsky, J., Kozlikova, B., Gora, A., Sustr, V., Klvana, M., Medek, P., Biedermannova, L., Sochor, J., and Damborsky, J. (2012) Caver 3.0: A tool for the analysis of transport pathways in dynamic protein structures. *PLoS Comput Biol* **8**, e1002708

FOOTNOTES

Funding: This work was financially supported by Syracuse University, American Diabetes Association grants #1-16-JDF-042 and #7-18-MUI-001 to JLH, and National Science Foundation grant CAREER CBET-1453312 to SN. KRMG was supported in part by an U.S. Department of Education GAANN Fellowship (P200A090277). This material is based in part upon work supported by the National Science Foundation under Grant No. CHE-1659775. The authors also gratefully acknowledge computational resources provided by Syracuse University research computing and the Extreme Science and Engineering Discovery Environment (XSEDE), which is supported by a National Science Foundation grant NSF ACI-1053575.

Abbreviations: MBOAT, membrane bound O-acyltransferase; GOAT, ghrelin O-acyltransferase; ER, endoplasmic reticulum; Hhat, Hedgehog acyltransferase; Porcn, Porcupine; hGOAT, human ghrelin O-acyltransferase; DltB, D-alanyl transferase DltB; TM, transmembrane; IM, intramembrane; RMSD, Root-mean-square deviation; CoA, coenzyme A; WT, wild type; C12, twelve carbon; C14, fourteen carbon; MSA, multiple sequence alignment; DPPC, dipalmitoylphosphatidylcholine; DOPC, dioleoyl phosphatidylcholine; NaCl, sodium chloride; MAFP, methoxy arachidonyl fluorophosphonate; DMSO, dimethyl sulfoxide; HA, human influenza hemagglutinin; EV, empty vector; PVDF, polyvinylidene difluoride; TBST, Tris-buffered saline, 0.1% Tween 20; HEPES, 4-(2-hydroxyethyl)-1-piperazineethanesulfonic acid; HPLC, high performance liquid chromatography; CMC, critical micelle concentration

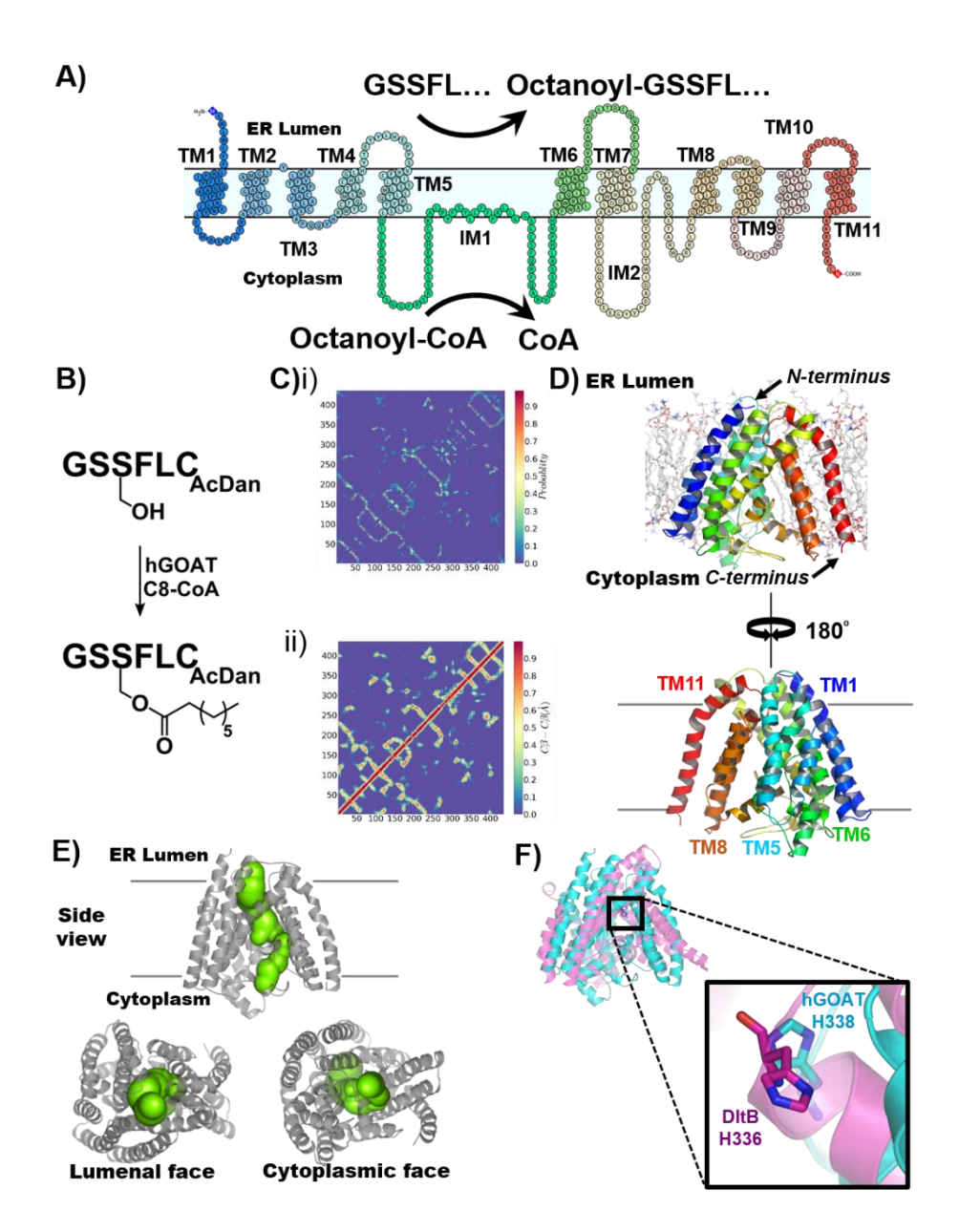


Figure 1. Structural model of hGOAT generated by computational methods. A) Schematic of ghrelin octanoylation by hGOAT showing the predicted transmembrane topology of hGOAT containing eleven transmembrane helix domains (TM1-11), two intramembrane domains (IM1-2), and loop regions generated using Protter.(43) B) Octanoylation of a ghrelin-mimetic fluorescent peptide by recombinant hGOAT. C) Contact maps for hGOAT showing the probability for a co-evolutionary contact from RaptorX analysis (i) and amino acid contacts in the final optimized hGOAT structure (ii). D) Structure of hGOAT in an ERmimetic lipid membrane, correlated to color-coded membrane topology in part a). E) Illustration of internal channel within hGOAT (green) transiting from the ER lumen to the cytoplasm, with the channel determined by CAVER 3.0 plugin in PyMOL.(52) F) Structural overlay of hGOAT and DltB showing the absolutely conserved histidine residues (hGOAT H338, teal; DltB H336, purple, PDB ID 6BUG:C) within these acyltransferases.

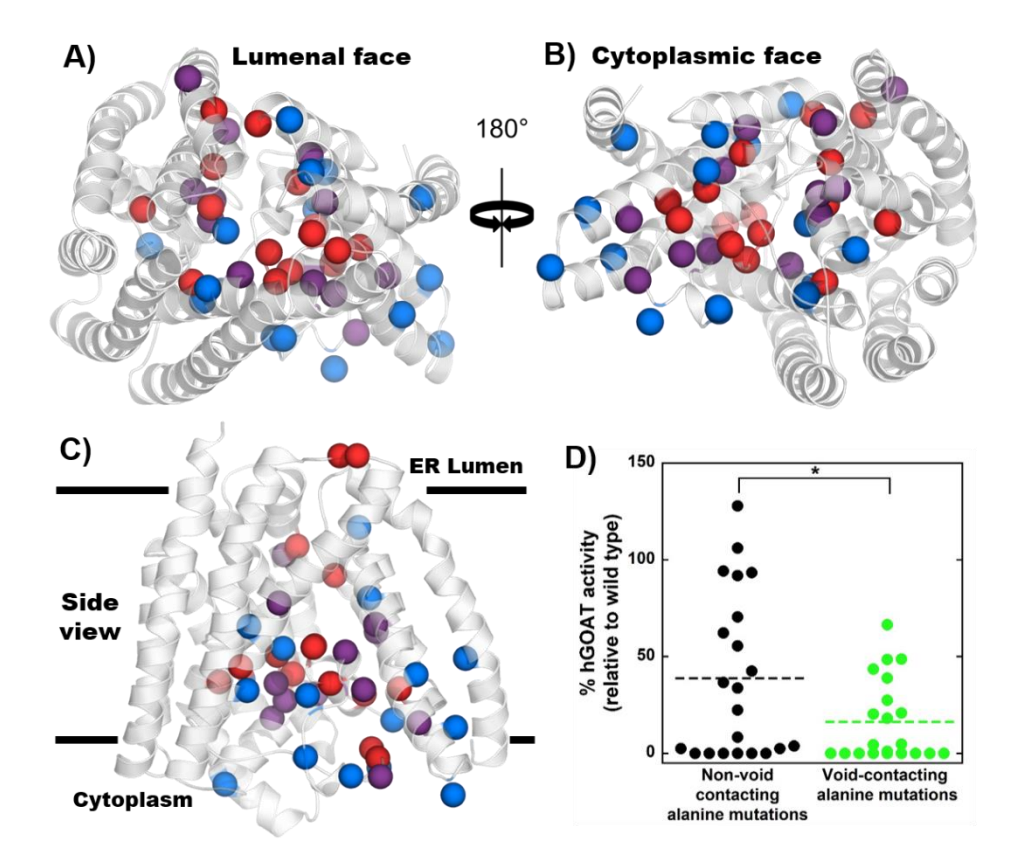


Figure 2. Mutagenesis studies support the location and functional importance of the hGOAT internal channel. A-C) Alanine mutations mapped onto the hGOAT structure, with each sphere denoting the alpha carbon of the mutated residue; spheres colored as follows: Blue, alanine variants with octanoylation activity within 3-fold of WT hGOAT; purple, alanine variants with impaired octanoylation activity (>3-fold loss compared to WT hGOAT); red, inactive alanine variants. A) View from lumenal face; B) view from cytoplasmic face; C) side view in the plane of the ER membrane. D) Octanoylation activity of hGOAT alanine variants for non-void contacting (black, N=21) and void-contacting mutations (green, N=21), with dotted lines denoting the average acylation activity for each group; *, p < 0.03.

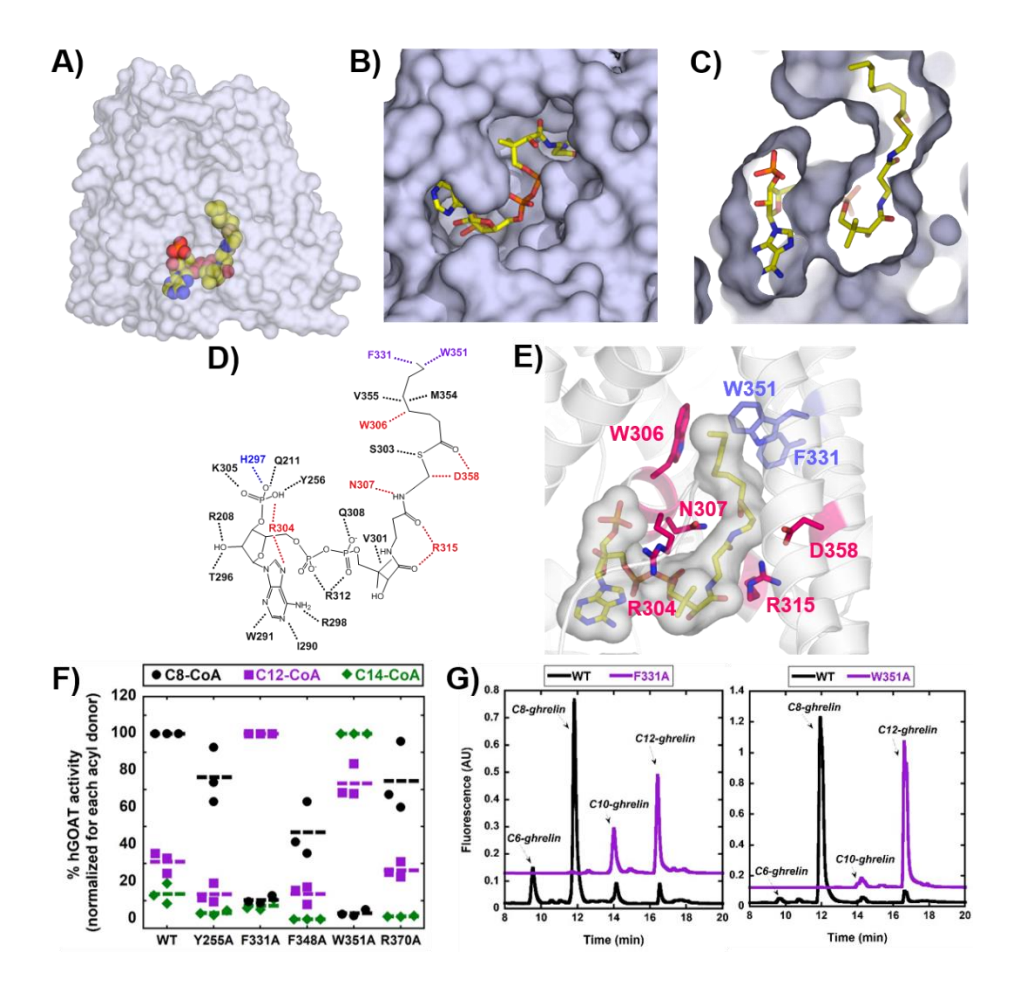


Figure 3. The acyl donor binding site within hGOAT. A) Structure of octanoyl-CoA bound within hGOAT from a side view in the plane of the ER membrane. B) View from the cytoplasmic face of hGOAT showing the solvent-exposed portions of the coenzyme A component of octanoyl-CoA. C) Cutaway view showing the acyl chain binding pocket within hGOAT, bent sharply upward from the coenzyme A binding regions on the cytoplasmic face of hGOAT. D) - E) Interactions between the octanoyl-CoA acyl donor and hGOAT residues; hGOAT residues shown in purple reduce acylation activity under standard reaction conditions when mutated to alanine, and residues shown in red abolish acylation activity upon alanine mutation. F) Acylation activity of WT hGOAT and selected hGOAT alanine variants using octanoyl-, lauryl-, or myristoyl-CoA as the sole acyl donor. Activities are normalized to the most reactive hGOAT variant with each acyl donor; individual data points indicate independent trials, and the dotted line indicates the average of three independent trials. G) Acyl donor competition demonstrates altered selectivity to a longer acyl donor for F331A and W351A hGOAT variants, consistent with the predicted interaction of these amino acid side chains with the distal end of the octanoyl acyl chain.

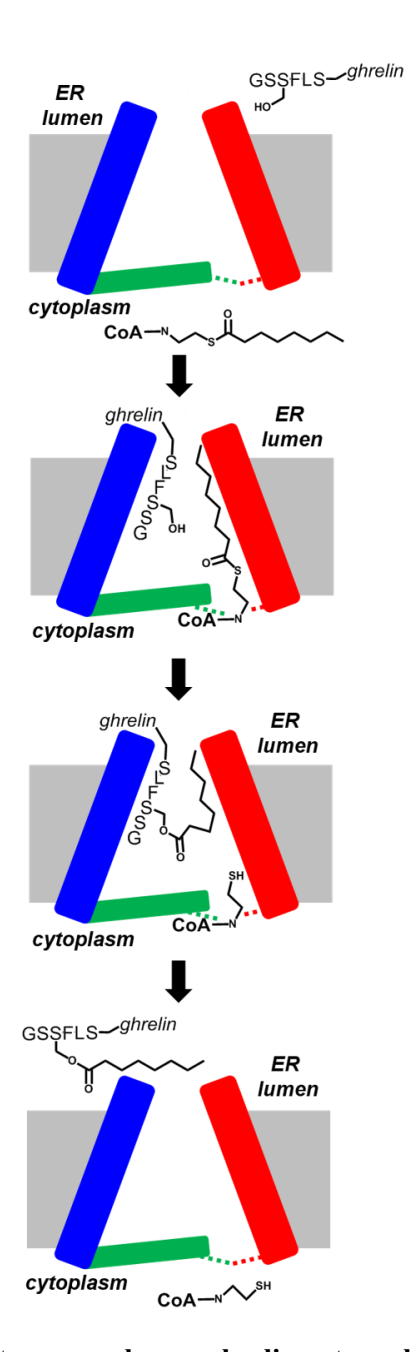


Figure 4. Proposed pathway for transmembrane ghrelin octanoylation by GOAT. Ghrelin (GSSFL-ghrelin) and octanoyl-CoA enter the GOAT internal channel from the ER lumenal pore and cytoplasmic acyl donor binding sites, respectively, followed by acyl transfer to the ghrelin serine side chain hydroxyl. Octanoylated ghrelin dissociates to the ER lumen resulting in the octanoyl chain transiting through the GOAT interior, and coenzyme A is released back to the cytoplasm. The red and blue rectangles represent perimeter helices, the green rectangle represents intramembrane domains forming the cytoplasmic surface of hGOAT, and dotted lines represent binding interactions between the octanoyl-CoA acyl donor and its binding site within hGOAT.

The ghrelin *O*-acyltransferase structure reveals a catalytic channel for transmembrane hormone acylation

Maria B Campaña, Flaviyan Jerome Irudayanathan, Tasha R Davis, Kayleigh R McGovern-Gooch, Rosemary Loftus, Mohammad Ashkar, Najae Escoffery, Melissa Navarro, Michelle A Sieburg, Shikha Nangia and James L Hougland

J. Biol. Chem. published online August 14, 2019

Access the most updated version of this article at doi: 10.1074/jbc.AC119.009749

Alerts:

- When this article is cited
- When a correction for this article is posted

Click here to choose from all of JBC's e-mail alerts